Biochemistry

 Volume 41, Number 18 May 7, 2002

Articles

Resonance Raman Detection of the Fe−S Bond in Endothelial Nitric Oxide Synthase[†,‡]

Johannes P. M. Schelvis,*[,§] Vladimir Berka,[||,⊥] Gerald T. Babcock,[⊥] and Ah-lim Tsai*[,||]

Department of Chemistry, New York University, New York, New York 10003, Department of Internal Medicine, Division of Hematology, University of Texas Medical School at Houston, Houston, Texas 77030, and Department of Chemistry and LASER Laboratory, Michigan State University, East Lansing, Michigan 48824

Received September 25, 2001; Revised Manuscript Received February 6, 2002

ABSTRACT: We report the first low-frequency resonance Raman spectra of ferric endothelial nitric oxide synthase (eNOS) holoenzyme, including the frequency of the Fe−S vibration in the presence of the substrate L-arginine. This is the first *direct* measurement of the strength of the Fe−S bond in NOS. The Fe−S vibration is observed at 338 cm^{-1} with excitation at 363.8 nm. The assignment of this band to the Fe−S stretching vibration was confirmed by the observation of isotopic shifts in eNOS reconstituted with ^{54}Fe- and ^{57}Fe-labeled hemin. Furthermore, the frequency of this vibration is close to those observed in cytochrome $P450_{cam}$ and chloroperoxidase (CPO). The frequency of this vibration is lower in eNOS than in $P450_{cam}$ and CPO, which can be explained by differences in hydrogen bonding to the proximal cysteine heme ligand. On addition of substrate to eNOS, we also observe several low-frequency vibrations, which are associated with the heme pyrrole groups. The enhancement of these vibrations suggests that substrate binding results in protein-mediated changes of the heme geometry, which may provide the protein with an additional tuning element for the redox potential of the heme iron. The implications of our findings for the function of eNOS will be discussed by comparison with $P450_{cam}$ and model compounds.

Nitric oxide synthase (NOS)[1] is a cytochrome P450 type enzyme, which is responsible for the physiological production of NO, an important signaling and immune response molecule (*1*−*5*). NOS converts L-arginine to L-citruline in two consecutive oxygenation steps. The enzyme has a reductase domain containing two flavin cofactors and an oxygenase domain binding one heme cofactor and a tetrahydrobiopterin (H_4B). The substrate binds in the distal heme pocket, while the oxygen reduction chemistry occurs at the heme iron. It has been recognized that the proximal heme ligand and proximal and distal side amino acid residues play an important role in the oxygen chemistry occurring in heme proteins. A "push−pull" mechanism was proposed for general peroxidases, in which the proximal ligand promotes

[†] This work was supported by grants from the NIH (GM 25480 to G.T.B. and GM 56818 to A.L.T. and V.B.) and start-up funds from New York University (to J.P.M.S.).

[‡] This paper is dedicated to the memory of Gerald T. Babcock.

* To whom correspondence should be addressed. J.P.M.S.: tel, (212) 998 3597; fax, (212) 260 0795; e-mail, Hans.Schelvis@nyu.edu. A.T.: tel, (713) 500 6771; fax, (713) 500 6810; e-mail, Ah-Lim.Tsai@uth.tmc.edu

[§] New York University.

[||] University of Texas Medical School at Houston.

[⊥] Michigan State University.

[1] Abbreviations: CBS, cystathionine β-synthase; CPO, chloroperoxidase; (e)NOS, (endothelial) nitric oxide synthase; EPR, electron paramagnetic resonance; P450, cytochrome P450; ν(Fe−His), iron−histidine stretching frequency; ν(Fe−S), iron−sulfur stretching frequency; 5c/hs, five-coordinate high spin; 6c/ls, six-coordinate low spin.

10.1021/bi0118456 CCC: $22.00
Published on Web 04/16/2002

O−O bond cleavage, the "push", and a distal side residue provides a "pull" as an acid−base catalyst or by polarizing the O−O bond (*6*). Recent studies of protein crystal structures and site-directed mutagenesis experiments, however, have challenged the role of the proximal ligand and the push−pull mechanism (*7*). The role of the proximal ligand in a nucleophilic-type electronic push is suggested to be less strong, but it would still play an important role in the stability of the Fe^{4+}═O intermediate (*7*). A correlation was observed between the strength of the Fe−His bond, as measured by the frequency of the Fe−His vibration [ν(Fe−His)], and the stabilization of specific oxygen reduction intermediates, especially Fe^{4+}═O (*8*). The strength of the Fe−His bond depends on the electron-donating power of the proximal histidine. The higher the basicity of the proximal histidine, as modulated by hydrogen bonding to its N_δ proton, the higher the Fe−His stretching frequency (*9*).

In NOS, the proximal heme ligand is a cysteine thiolate as in cytochrome P450 (*10*−*14*). The information about the strength of the Fe−S(Cys) bond in heme proteins is scarce. Since the vibrational frequency of the Fe−S vibration [ν(Fe−S)] can be used as a measure of the Fe−S bond strength, the determination of ν(Fe−S) for different heme proteins will contribute to insight into the role of the proximal ligand in the oxygen reduction chemistry. The frequency of ν(Fe−S) has been determined only for a few heme proteins: cytochrome P450, chloroperoxidase (CPO), and, recently, cystathionine β-synthase (CBS). In the first two proteins, ν(Fe−S) was determined for the high-spin (hs), five-coordinate (5c) ferric form of the heme cofactor at 351 and 347 cm^{-1}, respectively (*15*−*17*). In the latter protein, ν(Fe−S) was determined for the low-spin (ls), six-coordinate (6c) ferric form of the heme cofactor at 312 cm^{-1} (*18*). Although the interactions between NOS and exogenous ligands in the distal heme pocket have been investigated with resonance Raman spectroscopy (*19*−*25*), the interaction of NOS with its endogenous proximal heme ligand has not been reported, and the ν(Fe−S) frequency is not known. Therefore, we set out to determine this important parameter, i.e., ν(Fe−S), in the endothelial (e)NOS holoenzyme and by using eNOS reconstituted with hemin containing either the ^{54}Fe or the ^{57}Fe isotope.

MATERIALS AND METHODS

The eNOS holoenzyme was prepared as previously described with slight modifications (*26*). For expression of ^{54}Fe- or ^{57}Fe-labeled eNOS, Sf9 cells cultured in suspension were infected by recombinant baculoviruses at a multiplicity of infection of 2. Sepiapterin (10 μM) was added to the culture medium 24 h after infection, and ^{54}Fe- or ^{57}Fe-labeled hemin (2 μg/mL + 50 mL of serum per 500 mL cells cultured in suspension) was added 48 h after infection. The cells were harvested 72 h postinfection.

The resonance Raman spectra were obtained using a single spectrograph (TriAx 550, JY/Horiba) and a N_2(l)-cooled CCD detector (Spectrum One, JY/Horiba). For the isotope experiments a CCD detector with a 2000 × 800 pixel UV-enhanced chip (Site) was used, while the other spectra were recorded with a CCD detector with a UV-enhanced 2048 × 512 pixel chip (EEV). The Rayleigh scattering was removed by using appropriate holographic notch filters (Kaiser Optical). The experimental setup has been described in detail elsewhere (*27*). The samples were excited with either the 363.8 nm line from an Ar^+ laser (Coherent I-200 and I-307) or the 406.7 nm line from a Kr^+ laser (Coherent I-90 and I-302). The samples were placed in a spinning cell under an Ar atmosphere. The experiments were conducted at 6 ± 2 °C. Sample concentrations and laser energies are indicated in the figure legends. All spectra were corrected for the flavin fluorescence background, which was simulated by a polynomial function. The vibrational modes were labeled according to ref *28*, and the modes were assigned following in refs *29* and *30* unless indicated differently.

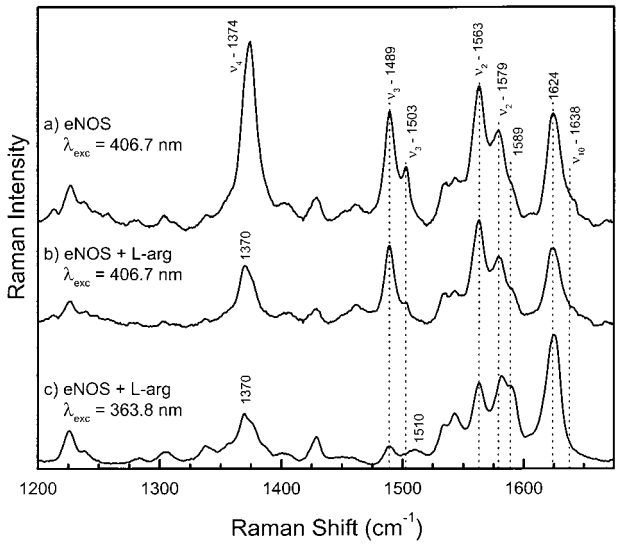

FIGURE 1: High-frequency resonance Raman spectrum of the eNOS holoenzyme (15 μM) as isolated in the absence (a) and presence (b, c) of 4 mM L-arginine. Excitation was at 406.7 nm (a, b) and 363.8 nm (c) with 10 mW power. The spectrum of the buffer was subtracted to remove contributions of glycerol.

RESULTS

The high-frequency resonance Raman spectra of the eNOS holoenzyme are shown in Figure 1. The spectrum of the eNOS holoenzyme as isolated, excited at 406.7 nm, Figure 1a, is characterized by vibrations at 1374, 1489, 1503, 1563, 1579, and 1624 cm^{-1}. These vibrations can be assigned to the heme skeletal vibrations that are indicative of the oxidation, coordination, and spin states of the heme iron (*28*−*30*). The oxidation state marker, ν_4, is observed at 1374 cm^{-1}. The ν_3, ν_2, and ν_{10} vibrations are particularly sensitive to the spin and coordination states of the heme iron. Two ν_3 vibrations can be assigned at 1489 and 1503 cm^{-1}. The ν_2 region, 1550−1600 cm^{-1}, is generally congested with contributions from other vibrations, e.g., ν_{11}, ν_{19}, and ν_{37}, which complicate the assignment of the ν_2 vibration. We assign the vibrations at 1563 and 1579 cm^{-1} to the ν_2 vibration (*31*). The strong vinyl stretching vibration, ν_{CC}, at 1624 cm^{-1} convolutes with the ν_{10} vibration. The shoulder around 1638 cm^{-1} can be assigned to ν_{10}. The observation of two ν_3 and ν_2 vibrations indicates that the heme of the eNOS holoenzyme as isolated is present in a mixture of five-coordinate (5c), high-spin (hs), and six-coordinate (6c), low-spin (ls) ferric heme. The ν_4, ν_3, ν_2, and ν_{10} vibrations at 1374, 1503, 1579, and 1638 cm^{-1}, respectively, are characteristic for the 6c/ls ferric heme, while the ν_3 and ν_2 vibrations

at 1489 and 1563 cm^{-1}, respectively, indicate a 5c/hs heme. The ν_4 and ν_{10} vibrations corresponding to the 5c/hs ferric heme are hidden under the 1374 cm^{-1} ν_4 (6c/ls) vibration and the 1624 cm^{-1} ν_{CC} vibration, respectively. The observation of the mixed heme spin states in eNOS is in agreement with EPR experiments on eNOS (*32*). Addition of the substrate L-arginine to the eNOS holoenzyme induces considerable changes in its resonance Raman spectrum (Figure 1b). The ν_4 vibration shifts to 1370 cm^{-1} with a small high-frequency shoulder at 1374 cm^{-1} on addition of L-arginine. The intensity of the ν_3 vibration at 1503 cm^{-1}, indicative of the low-spin species, is significantly reduced in the presence of substrate. No dramatic changes are observed in the congested ν_2 region, and the ν_{10} vibration at 1638 cm^{-1} is barely detectable after addition of the substrate. The Raman spectrum of eNOS in the presence of L-arginine indicates that the addition of substrate induces the formation of the ferric 5c/hs heme in eNOS, as judged from the coordination and spin state marker bands, $\nu_3 = 1489$ cm^{-1} and $\nu_2 = 1563$ cm^{-1}. The shift of the ν_4 vibration to 1370 cm^{-1} supports this assignment, which is in agreement with previous EPR, UV−vis, and Raman results (*12*, *23*, *26*, *32*). The presence of a few weak vibration associated with a 6c/ls ferric heme is due to a small population of hemes ($\lambda_{max} =$ 400 nm), which is relatively more enhanced with 406.7 nm excitation than the 5c/hs hemes ($\lambda_{max} = 394$ nm) (*26*). The change in spin and coordination states of the heme iron after addition of substrate has been observed in P450, rat brain NOS, and (e)NOS (*21*, *23*, *26*, *33*). When 363.8 nm excitation is used, the Raman vibrations of the 5c/hs ferric heme species of eNOS are strongly enhanced. The resonance Raman spectrum of eNOS in the presence of L-arginine excited at this wavelength is shown in Figure 1c. The excitation of heme molecules with near-UV light enhances nontotally symmetric vibrations. Totally symmetric vibrations such as ν_4, ν_3, and ν_2 are observed at decreased intensities with respect to excitation at 406.7 nm (see Figure 1b). They are observed at 1370, 1489, and 1563 cm^{-1}, respectively. The vibrations at 1589 and 1510 cm^{-1} are assigned to the ν_{37} and ν_{38} vibrational modes, respectively. The apparent shift of the 1579 cm^{-1} vibration to 1582 cm^{-1} is most likely caused by UV enhancement of the ν_{19} vibrational mode and disappearance of the ν_2 vibration associated with the 6c/ls ferric heme. The vibration at 1625 cm^{-1} is strongly polarized (data not shown), and we assign it to the ν_{CC} vibration. Its apparent shift may be induced by the underlying ν_{10} vibration, which is enhanced with near-UV excitation. This is in contrast with P450, in which the ν_{10} vibration was strongly enhanced with 363.8 nm excitation and dominated the 1623 cm^{-1} vibration (*31*). The high-frequency shoulder on the ν_4 vibration is also observed for near-UV excitation of P450, but an assignment cannot be made at this moment (*31*).

The first low-frequency spectrum of the ferric eNOS, actually of any ferric NOS, holoenzyme is shown in Figure 2. The spectrum obtained with 406.7 nm excitation is given in Figure 2a. This part of the Raman spectrum is characterized by the ν_7 and ν_8 vibrations, which are observed at 678 and 347 cm^{-1}, respectively. A shoulder around 325 cm^{-1} can be discerned at the low-frequency side of the ν_8 vibration. Addition of L-arginine to eNOS does induce some changes in the low-frequency spectrum as shown in Figure 2b. This part of the Raman spectrum is usually not particularly

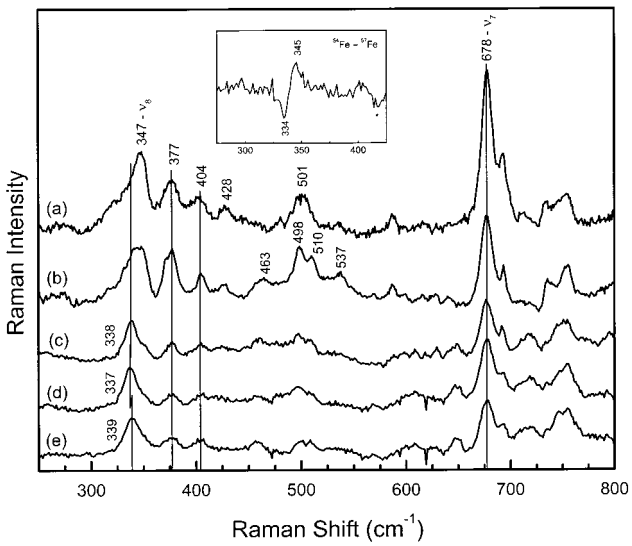

FIGURE 2: Low-frequency resonance Raman spectra of eNOS. (a) eNOS holoenzyme as isolated (20 μM) and (b) eNOS holoenzyme (15 μM) in the presence of 4 mM L-arginine excited at 406.7 nm, 10 mW. (c) eNOS holoenzyme (15 μM) in the presence of 4 mM L-arginine excited at 363.8 nm, 10 mW. eNOS (10 μM) reconstituted with hemin-^{57}Fe (d) or hemin-^{54}Fe (e) in the presence of 100 μM L-arginine excited at 363.8 nm, 8 mW. The spectrum of the buffer was subtracted to remove contributions of glycerol. Inset: Difference spectrum of eNOS-^{54}Fe − eNOS-^{57}Fe. Some residual contributions of glycerol have been indicated with an asterisk.

sensitive to a change from 6c/ls to 5c/hs of ferric heme (*31*). Several changes can be observed, however, after addition of substrate. Two new vibrations are observed at 463 and 537 cm^{-1}, and the band at 501 cm^{-1} splits into two new vibrations at 498 and 510 cm^{-1}. The assignment of these vibrations is not straightforward, but a comparison to metmyoglobin can be made (*34*). The band at 463 cm^{-1} is most likely due to ν_{33}, a pyrrole rotational mode, and the band at 537 cm^{-1} can be assigned to γ_{21}, a symmetric pyrrole folding mode. The vibrations around 500 cm^{-1} are probably due to pyrrole swivel modes, e.g., γ_{12}. The enhancement/activation of these pyrrole modes on addition of substrate to eNOS was unexpected and may provide additional information about the regulation of enzyme activity by small structural adjustments of the protein and the heme cofactor.

The Fe−S vibration in P450 was observed in the presence of substrate and excitation at 363.8 nm in the Fe−S charge-transfer band (*35*). Under similar conditions, i.e., in the presence of L-arginine to form 5c/hs eNOS and with excitation at 363.8 nm, the low-frequency spectrum of eNOS was obtained (Figure 2c). This spectrum shows the ν_7 vibration at 678 cm^{-1}, and the weaker vibrations at 377 and 404 cm^{-1} were also observed. The ν_8 vibration was not observed with 363.8 nm excitation. Instead, a new vibration at 338 cm^{-1} was present, which was absent upon excitation with 406.7 nm excitation. The disappearance and appearance of these vibrations at different excitation wavelengths were observed before in P450 (*31*). Excitation at the low-energy side of the Soret band results in enhancement of porphyrin skeletal vibrations such as ν_8 (*35*). Excitation at the high-energy side of the Soret band yields enhancement of the Fe−S vibration due to the presence of an Fe−S charge-transfer band at the high-energy side of the Soret absorption band (*35*). The new vibration at 338 cm^{-1} could be the Fe−S stretching vibration of 5c/hs ferric eNOS. To verify this

Table 1: Heme Skeletal[a] and Fe−S Vibrations of Ferric Heme Proteins with a Cysteine as the Proximal Heme Ligand

	ν_4	ν_3	ν_2	ν_{10}	ν(Fe−S)	state	ref
eNOS	1370	1489	1563	nd[b]	338	5c/hs	this work
eNOS	1370	1488	1562	nd[b]		5c/hs	*23*
b-NOS[c]	1370	1487	1563	1623		5c/hs	*19*
P450	1368	1488	1570	1623	351	5c/hs	*15*, *31*
CPO	1369	1490	1567	nd[b]	347	5c/hs	*16*, *36*
eNOS	1374	1503	1579	1638		6c/ls	this work
eNOS	1373	1500	1578	1635		6c/ls	*23*
b-NOS[c]	1371	1502	1575	nd[b]		6c/ls	*21*
P450	1372	nd[b]	1582	1637		6c/ls	*31*
CPO	1373	1504	nd[b]	1640		6c/ls	*35*
CBS	1372	1500	1575	1630	312	6c/ls	*18*

[a] Vibrational mode labeling and assignment according to refs *28*−*30*; frequencies are given in cm^{-1}. [b] nd is not determined. [c] b-NOS is rat brain NOS.

tentative assignment, we reconstituted eNOS with isotopically labeled hemin, ^{54}Fe and ^{57}Fe. Excitation both at 406.7 nm and at 363.8 nm of the reconstituted eNOS samples indicated that the heme was ferric, 5c/hs (data not shown). The low-frequency resonance Raman spectra of the isotopically labeled eNOS in the presence of 100 μM L-arginine and excited at 363.8 nm are shown in spectra d and e of Figure 2 for ^{57}Fe and ^{54}Fe, respectively. For both isotopes, the ν_7 vibration is observed at the same frequency as in the holoenzyme at 678 cm^{-1}. Also, the vibrations at 377 and 404 cm^{-1} are not affected by the Fe isotope substitution. The vibration at 338 cm^{-1}, however, does show an isotopic shift. For the ^{57}Fe sample (Figure 2d), this vibration is now observed at 337 cm^{-1}, while it has a frequency of 339 cm^{-1} for the ^{54}Fe sample (Figure 2e). In the inset, the difference spectrum is shown from 275 to 425 cm^{-1}. The isotopic shifts are very reproducible for different samples. In contrast, no isotopic shift was detected in the low-frequency spectrum when 406.7 nm light was used for excitation (data not shown).

DISCUSSION

Spin and Coordination States of the eNOS Holoenzyme. The resonance Raman spectrum presented in Figure 1a and the frequencies tabulated in Table 1 indicate that the ferric heme of the eNOS holoenzyme as isolated is present in a mixture of 5c/hs and 6c/ls. The observation of the mixed hemes in eNOS is in agreement with EPR experiments on eNOS (*32*). Raman experiments on NOS and P450 also showed a mixture of 5c/hs and 6c/ls ferric hemes (*19*, *21*, *23*, *31*, *33*). NOS can also form a P420-like, inactive enzyme, which is 6c/ls (*21*). We can rule out that this form is present in our samples. First, the electronic spectrum of CO−ferrous eNOS shows that the 6c/ls heme species is not due to an inactive P420-like eNOS (*37*). Second, it is common for 6c/ls ferric P450, rat brain NOS, and (e)NOS to be converted to a 5c/hs ferric heme species by the addition of substrate (*21*, *23*, *26*, *33*). Third, the vibration at 428 cm^{-1} in the low-frequency spectrum of eNOS holoenzyme (Figure 2a) supports our conclusion that the 6c/ls heme species of eNOS in our sample is active enzyme, because for inactive P420-like enzyme, this vibration would be expected at a lower frequency, i.e., 418 cm^{-1} (*31*). Therefore, we conclude that both the 5c/hs and 6c/ls species of eNOS in our samples are active forms of the enzyme and that the 6c/ls species can be converted into the 5c/hs species by addition of substrate to the sample.

Effect of L-Arginine Binding on Low-Frequency Vibrations. In this paper, we report for the first time the low-frequency Raman spectra of a ferric NOS holoenzyme, eNOS in our case. The addition of L-arginine to the eNOS holoenzyme seems to have a small effect on the low-frequency Raman spectrum (Figure 2a,b). This is not too surprising because the low-frequency vibrations are less sensitive to the change in spin and coordination states. Several small changes, however, need further discussion. On addition of L-arginine, two new vibrations appear at 463 and 537 cm^{-1}. Furthermore, the band at 501 cm^{-1}changes shape after addition of the substrate and splits into two vibrations at 498 and 510 cm^{-1}. We have assigned these bands to vibrational modes related to the pyrrole groups. Apparently, addition of substrate to the eNOS holoenzyme results in the activation or enhancement of these modes. This suggests that substrate binding induces a geometrical change of the heme cofactor. Since the substrate binds in the distal heme pocket and does not directly interact with the heme cofactor, a small protein perturbation will have to occur on substrate binding, which affects the heme geometry. This protein-mediated change in heme geometry may be related to the change in rhombicity of the EPR signal, which is observed on binding of substrate and other type I ligands in the eNOS distal heme pocket (*32*). An effort to test the hypothesis of a correlation between the rhombicity of the EPR signal and the low-frequency vibrations in the Raman spectrum is currently underway. Furthermore, it was shown that the redox potential of the heme iron in iNOS and nNOS is raised by 32 and 9 mV, respectively, on addition of L-arginine. Although the redox potential of the heme iron in eNOS is not yet known, we assume that it may display a similar behavior as observed in iNOS and nNOS on addition of substrate. Our observation of a change in heme geometry to eNOS may indicate a structural basis for the change in the redox potential on addition of L-arginine (*38*).

Detection of the Fe−S Vibration. The low-frequency spectra of eNOS obtained with 406.7 nm excitation in the presence and absence of substrate did not show many differences (Figure 2a,b). The main vibrations are the ν_7 and ν_8 modes at 678 and 347 cm^{-1}, respectively. The low-frequency spectrum of eNOS in the presence of substrate obtained with 363.8 nm excitation does show a few differences from those obtained with 406.7 nm excitation (Figure 2c). Although the ν_7 vibration and the vibrations at 377 and 404 cm^{-1} are still observed, the ν_8 vibration is absent, and a new vibration is observed at 338 cm^{-1} on excitation with 363.8 nm. With this excitation wavelength, the Fe−S vibration, which had previously been detected in P450 and CPO, emerged (*15*−*17*). Our tentative assignment of the 338 cm^{-1} vibration to the Fe−S vibration of eNOS is confirmed by the observation of the isotopic shift of this vibration in eNOS reconstituted with either ^{57}Fe- or ^{54}Fe-labeled hemin (spectra d and e of Figure 2, respectively). The small isotopic shift of about 2 cm^{-1} is clearer in the isotope difference spectrum shown in the inset of Figure 2. In P420, a weak, broad vibration can be observed at 340 cm^{-1} on excitation at 363.8 nm, which may be due to an altered Fe−S geometry with respect to P450 (*31*). In our samples, the high-frequency spectrum of eNOS in the presence of substrate (Figure 1c),

however, indicates that we are detecting the ferric 5c/hs form of the active enzyme on excitation with 363.8 nm and not an inactive P420 type of enzyme. Therefore, we conclude that the ferric 5c/hs, active form of eNOS has an Fe−S vibration with a frequency of 338 cm^{-1}.

Implications of the Small Isotopic Shift. The shift of about 2 cm^{-1} in the Fe−S vibration in eNOS reconstituted with isotopically labeled hemin is similar to the isotopic shift that was observed for the Fe−S vibration in $P450_{cam}$, which was 2.5 cm^{-1} for ^{56}Fe- and ^{54}Fe-enriched samples (*15*). With a simple diatomic harmonic oscillator calculation for the Fe−S bond, we find an isotopic shift of 3.4 cm^{-1} for the ^{54}Fe and ^{57}Fe isotopes, which is larger than the observed shift. Champion and co-workers have pointed out that, in the case of P450, a three-body harmonic oscillator should be used, which takes into account coupling between the Fe−S and C−S vibrations (*15*). In these calculations, the parameters are the Fe−S−C angle (θ) and the force constants, k_1 and k_2, of the Fe−S and the C−S bonds, respectively. The angle θ varies from 100° to 123° in eNOS crystal structures (*39*, *40*). This results in a calculated isotopic shift ranging from 2.7 cm^{-1} for $\theta = 100°$ and $k_2 = 0.5k_1$ to 3.5 cm^{-1} for $\theta = 123°$ and $k_2 = 2k_1$. It is expected that the force constants lie in the range from $k_2 = k_1$ to $k_2 = 2k_1$ (*15*). In this range, the calculated isotopic shift varies from 3.3 to 3.5 cm^{-1}. The observed isotopic shift is still smaller than the calculated shift after taking into account coupling between the Fe−S and C−S vibrations.

It is possible that the force constants of Fe−S and C−S are significantly different, and coupling between the Fe−S and C−S vibrations does not occur. In that case, other bonds may be contributing to the 338 cm^{-1} vibration. The Fe−N(pyr) out-of-plane motion has a force constant that is comparable to that of Fe−N(His) (*41*) and, presumably, close to that of Fe−S(Cys). The eNOS crystal structures show that the heme is significantly distorted with the heme iron well out of the heme plane (*39*, *40*), and our current results indicate that addition of L-arginine to eNOS may result in changes of the heme geometry. This suggests that the Fe−N(pyr) bond could potentially contribute to the 338 cm^{-1} vibration, decreasing the sensitivity of the vibration to Fe isotopes and lowering the actual isotopic shift. It has been shown in the myoglobin mutant H93G that calculations of the isotopic shift of the Fe−Im stretching frequency that include the pyrrole nitrogens are significantly closer to the experimental value. Although inclusion of all atoms is even better, none of the two models fitted all the data perfectly, and it was concluded that anharmonic coupling was a complicating factor (*41*). To perform calculations on the Fe−S isotopic shift that include more atoms, more isotopic data would be required and is currently not feasible.

Comparison to P450, CPO, and Model Compounds. The Fe−S stretching frequency, 338 cm^{-1}, of eNOS is lower than that of $P450_{cam}$ and CPO, which are observed at 351 and 347 cm^{-1}, respectively. In the H25C mutant of heme oxygenase (HO), ν(Fe−S) is observed at 347.5 cm^{-1} (*42*). This indicates that the basicity of the cysteine thiolate in eNOS is lower than in P450 and CPO and also lower than in the HO proximal heme−ligand mutant H25C. A comparison of the crystal structures of eNOS, P450, and CPO shows that the proximal thiolates of P450 and CPO accept hydrogen bonds from two peptide NH groups (*43*−*45*). In eNOS, the proximal thiolate accepts a hydrogen bond from a peptide NH group and an indole nitrogen proton of a Trp residue (*39*, *46*). From these data and from resonance Raman experiments on the NOS−CO complex, it was suggested that the basicity of the proximal thiolate in NOS is lower than that in P450 and CPO (*22*). The EPR data of the low-spin eNOS complex also show smaller ligand field strength than that of $P450_{cam}$ but are comparable to that of low-spin CPO complexes (*32*). Now, we have directly measured the strength of the Fe−S bond in eNOS, as determined by the frequency of the Fe−S stretching vibration, and unambiguously proven that it is weaker than in P450 and CPO. Hence, the basicity of the proximal thiolate is lower in eNOS than in P450 and CPO.

Hydrogen bond formation to the thiolate of the proximal cysteine, however, is probably not the only factor regulating the basicity of the thiolate group and, thereby, the redox potential of the heme iron. Iron−porphyrin model compound studies have shown that hydrogen bonding to a proximal alkanethiolate group results in a shift to shorter wavelength of the Soret absorption of the ferrous CO complex and an increase in the redox potential of the heme iron, indicating an electron deficiency of the hydrogen-bonded thiolate (*47*). The same effect is observed for eNOS and P450 with absorption of the ferrous CO complexes at 444 and 447 nm, respectively (*48*, *49*), and redox potentials of the heme iron of −0.25/−0.26 V (nNOS/iNOS in the presence of H_4B and L-arg) and −0.42 V ($P450_{cam}$), respectively (*38*, *50*). This also indicates electron deficiency of the thiolate of eNOS relative to that of P450, in agreement with more hydrogen bonding to the thiolate in eNOS. The analogy between the model compounds and enzymes breaks down when the ν(Fe−S) frequency and the Fe−S bond length are considered. In the model compounds, hydrogen bond formation to the thiolate results in a *higher* ν(Fe−S) frequency and a *shorter* Fe−S bond length. The opposite change is observed for the enzymes; an increase in hydrogen bonding gives rise to a *lower* ν(Fe−S) frequency (Table 1) and a *longer* Fe−S bond length, 2.22−2.25 and 2.20 Å for eNOS (in the presence of H_4B and L-arg) and $P450_{cam}$, respectively (*13*, *39*, *40*). We cannot explain the discrepancy between the enzymes and the model compounds. The data for the enzymes are self-consistent, but those for the model compounds are not. Most likely, the model compounds do not mimic the protein environment well. It is possible that the substituent groups of the porphyrin ring and of the axial ligand of the model compounds may affect the electron densities on the heme iron and the thiolate, respectively, and potentially obscure the effect of hydrogen bond formation. In addition, the scaffolding that holds the thiolate ligation may force a short Fe−S bond length on the model compounds.

The lower ν(Fe−S) frequency in eNOS relative to P450 seems logical given the lower electron density on the thiolate of eNOS, which is expected to result in a weaker Fe−S bond and, therefore, in a lower ν(Fe−S) frequency. The protein environment of the heme in eNOS and P450, however, may play a more complex role in tuning the redox potential of the heme iron than just providing hydrogen bonds to the thiolate. Heme nonplanarity also affects the redox potential of the heme iron (*51*). From the crystal structures it is clear that both eNOS and P450 have nonplanar hemes (*13*, *39*, *40*). The heme in eNOS is significantly more distorted than

the heme in P450. Furthermore, our low-frequency Raman data indicate that an additional, protein-mediated change in the heme geometry occurs after addition of L-arginine. Therefore, the observed difference in the strength of the Fe−S bond between eNOS and P450 as measured by the ν(Fe−S) stretching frequency is most likely due to a combination of protein-mediated effects, i.e., hydrogen bond formation to the thiolate of the cysteine proximal heme ligand and heme distortion. Additional hydrogen bond formation to the thiolate and significant nonplanarity of the heme in eNOS result in electron deficiency of the thiolate and the heme iron with respect to P450. This explains the weaker Fe−S bond in eNOS compared to P450 as determined from the ν(Fe−S) frequency. It also explains the higher redox potential of the heme iron in eNOS relative to P450 (ΔE_m = 0.17 V).

Unfortunately, there is currently not sufficient information available in the literature to investigate possible correlations between the ν(Fe−S) frequency, the low-frequency pyrrole vibrations, and functional properties of the P450-type enzymes, e.g., the redox potential. The Fe−S vibration has been determined for only three different enzymes with a 5c/hs heme, and assignment and interpretation of porphyrin vibrations in the 450−550 cm^{-1} region and their enhancement are very difficult. This prevents the correlation of these vibrations to a well-defined geometrical change of the heme cofactor. Furthermore, only a few oxygen-related vibrations have been determined for these three enzymes (*25*, *52*−*57*), and a full analysis of the effect of the proximal thiolate on the reactivity of oxygen intermediates, as for histidine (*8*), is not yet possible. To obtain the same level of knowledge as for proximal histidine-liganded heme proteins and for correlation of the vibrational data to geometrical changes, it is important that more data become available, not only for the NOS isoforms but also for other heme thiolate enzymes.

Conclusion. We have detected the Fe−S vibration at 338 cm^{-1} in eNOS in the presence of L-arginine. The frequency of this vibration is lower in eNOS than in P450 and CPO. Therefore, the Fe−S bond is weaker in eNOS than in the other two enzymes. We attribute the weaker Fe−S bond in eNOS to additional hydrogen bond formation to the proximal cysteine, which results in an electron deficiency of the thiolate. Hydrogen bond formation, however, is not the only contributing factor to the weakening of the Fe−S bond. The observation of low-frequency, pyrrole vibrational modes on addition of L-arginine to eNOS indicates that a protein-mediated change of the heme geometry may occur. Changes in the heme geometry have been linked to changes in the redox potential of heme irons. Therefore, reduction of the electron density of the heme iron can lead to an additional weakening of the Fe−S bond. Both hydrogen bonding to the thiolate and nonplanarity of the heme may also play important roles in elevating the redox potential of the heme iron in (e)NOS compared to P450. If this is the case, a correlation may exist between the ν(Fe−S) frequency and the redox potential of the heme iron in P450-type enzymes. More data, however, will be required before such a relationship can be corroborated.

ACKNOWLEDGMENT

The preliminary data in this study were obtained at Michigan State University.

REFERENCES

1. Kerwin, J. F., Jr., Lancaster, J. R., Jr., and Feldman, P. L. (1995) *J. Med. Chem. 38*, 4343−4358.
2. Feldman, P. L., Griffith, O. W., and Stuehr, D. J. (1993) *Chem. Eng. News 71*, 26−38.
3. Raman, C. S., Martasek, P., and Masters, B. S. S. (2000) in *The Porphyrin Handbook* (Kadish, K M., Smith, K. M., and Guilard, R., Eds.) Vol. 4, pp 293−327, Academic Press, New York.
4. McMillan, K., Bred, D. S., Hirsch, D. J., Snyder, S. H., Clark, J. E., and Masters, B. S. S. (1992) *Proc. Natl. Acad. Sci. U.S.A. 89*, 11141−11145.
5. White, K. A., and Marletta, M. A. (1992) *Biochemistry 31*, 6627−6631.
6. Dawson, J. H. (1988) *Science 240*, 433−439.
7. Poulos, T. (1996) *J. Biol. Inorg. Chem. 1*, 356−359.
8. Oertling, W. A., Kean, R. T., Wever, R., and Babcock, G. T. (1990) *Inorg. Chem. 29*, 2633−2645.
9. Teraoka, J., and Kitagawa, T. (1981) *J. Biol. Chem. 256*, 3969−3977.
10. Chen, P.-F., Tsai, A.-L., and Wu, K. K. (1994) *J. Biol. Chem. 269*, 25062−25066.
11. Richards, M. K., and Marletta, M. A. (1994) *Biochemistry 33*, 14723−14732.
12. McMillan, K., and Masters, B. S. S. (1995) *Biochemistry 34*, 3686−3693.
13. Poulos, T. L., Finzel, B. C., and Howard, A. J., (1987) *J. Mol. Biol. 195*, 697−700.
14. Dawson, J. H., and Sono, M. (1987) *Chem. Rev. 87*, 1255−1276.
15. Champion, P. M., Stallard, B. R., Wagner, G. C., and Gunsalus, I. C. (1982) *J. Am. Chem. Soc. 104*, 5469−5472.
16. Bangcharoenpaurpong, O., Hall, K. S., Hager, L. P., and Champion, P. M. (1986) *Biochemistry 25*, 2374−2378.
17. Yu, N.-T. (1986) *Methods Enzymol. 130*, 350−409.
18. Green, E. L., Taoka, S., Banerjee, R., and Loehr, T. M. (2001) *Biochemistry 40*, 459−463.
19. Wang, J., Stuehr, D. J., Ikeda-Saito, M., and Rousseau, D. L. (1993) *J. Biol. Chem. 268*, 22255−22258.
20. Wang, J., Rousseau, D. L., Abu-Soud, H. M., and Stuehr, D. J. (1994) *Proc. Natl. Acad. Sci. U.S.A. 91*, 10512−10516.
21. Wang, J., Stuehr, D. J., and Rousseau, D. L. (1995) *Biochemistry 34*, 7080−7087.
22. Wang, J., Stuehr, D. J., and Rousseau, D. L. (1997) *Biochemistry 36*, 4595−4606.
23. Rodríguez-Crespo, I., Moënne-Loccoz, P., Loehr, T. M., and Ortiz de Montellano, P. R. (1997) *Biochemistry 36*, 8530−8536.
24. Fan, B., Wang, J., Stuehr, D. J., and Rousseau, D. L. (1997) *Biochemistry 36*, 12660−12665.
25. Couture, M., Stuehr, D. J., and Rousseau, D. L. (2000) *J. Biol. Chem. 275*, 3201−3205.
26. Berka, V., Chen, P. F., and Tsai, A.-L. (1996) *J. Biol. Chem. 271*, 33293−33300.
27. Schelvis, J. P. M., Seibold, S. A., Cerda, J. F., Garavito, R. M., and Babcock, G. T. (2000) *J. Phys. Chem. B 104*, 10844−10850.
28. Abe, M., Kitagawa, T., and Kyogoku, Y. (1978) *J. Chem. Phys. 69*, 4256−4534.
29. Choi, S., and Spiro, T. G. (1983) *J. Am. Chem. Soc. 105*, 3683−3692.
30. Choi, S., Lee, J. J., Wei, Y. H., and Spiro, T. G. (1983) *J. Am. Chem. Soc. 105*, 3692−3707.
31. Wells, A. V., Li, P., Champion, P., Martinis, S. A., and Sligar, S. G. (1992) *Biochemistry 31*, 4384−4393.
32. Tsai, A.-L., Berka, V., Chen, P.-F., and Palmer, G. (1996) *J. Biol. Chem. 271*, 32563−32571.
33. Abu-Soud, H. M., Wang, J., Rousseau, D. L., and Stuehr, D. J. (1999) *Biochemistry 38*, 12446−12451.
34. Hu, S., Smith, K. M., and Spiro, T. G. (1996) *J. Am. Chem. Soc. 118*, 12638−12646.

35. Bangcharoenpaurpong, O., Champion, P. M., Martinis, S. A., and Sligar, S. G. (1987) *J. Chem. Phys. 87*, 4273−4284.
36. Remba, R. D., Champion, P. M., Fitchen, D. B., Chiang, R., and Hager, L. P. (1979) *Biochemistry 18*, 2280−2290.
37. Chen, P.-F., Tsai, A.-L., Berka, V., and Wu, K. K. (1997) *J. Biol. Chem. 272*, 6114−6118.
38. Presta, A., Weber-Main, A. M., Stankovich, M. T., and Stuehr, D. J. (1998) *J. Am. Chem. Soc. 120*, 9460−9465.
39. Raman, C. S., Li, H., Martasek, P., Kral, V., Masters, B. S., and Poulos, T. L. (1998) *Cell 95*, 939−950.
40. Fischmann, T. O., Hruza, A., Xiao, D. N., Fossetta, J. D., Lunn, C. A., Dolphin, E., Prongay, A. J., Reichert, P., Lundell, D. J., Narula, S. K., and Weber, P. C. (1999) *Nat. Struct. Biol. 6*, 233−242.
41. Franzen, S., Boxer, S. G., Dyer, R. B., and Woodruff, W. H. (2000) *J. Phys. Chem. B 104*, 10359−10367.
42. Liu, Y., Moënne-Loccoz, P., Hildebrand, D. P., Wilks, A., Loehr, T. M., Mauk, A. G., and Ortiz de Montellano, P. R. (1999) *Biochemistry 38*, 3733−3743.
43. Poulos, T. L., Finzel, B. C., Gunsalus, I. C., Wagner, G. C., and Kraut, J. (1985) *J. Biol. Chem. 260*, 16122−16130.
44. Schlichting, I., Berendzen, J., Chu, K., Stock, A. M., Maves, S. A., Benson, D. E., Sweet, R. M., Ringe, D., Petsko, G. A., and Sligar, S. G. (2000) *Science 287*, 1615−1622.
45. Sundaramoorthy, M., Terner, J., and Poulos, T. L. (1995) S*tructure 3*, 1367−1377.
46. Crane, B. R., Arvai, A. S., Gachhui, R., Wu, C., Ghosh, D. K., Getzoff, E. D., Stuehr, D. J., and Tainer, J. A. (1997) *Science 278*, 425−431.
47. Suzuki, N., Higuchi, T., Urano, Y., Kikuchi, K., Uekusa, H., Ohashi, Y., Uchida, T., Kitagawa, T., and Nagano, T. (1999) *J. Am. Chem. Soc. 121*, 11571−11572.
48. Chen, P. F., Tsai, A. L., Berka, V., and Wu, K. K. (1996) *J. Biol. Chem. 271*, 14631−14635.
49. Hanson, L. K., Eaton, W. A., Sligar, S. G., Gunsalus, I. C., Gouterman, M., and Connell, C. R. (1976) *J. Am. Chem. Soc. 98*, 2672−2674.
50. Fisher, M. T., and Sligar, S. G. (1985) *J. Am. Chem. Soc. 107*, 5018−5019.
51. Ma, J.-G., Zhang, J., Franco, R., Jia, S.-L., Moura, I., Moura, J. J. G., Kroneck, P. M. H., and Shelnutt, J. A. (1998) *Biochemistry 37*, 12431−12442.
52. Bangcharoenpaurpong, O., Rizos, A. K., Champion, P. M., Jollie, D., and Sligar, S. G. (1986) *J. Biol. Chem. 261*, 8089−8092.
53. Egawa, T., Ogura, T., Makino, R., Ishimura, Y., and Kitagawa, T. (1991) *J. Biol. Chem. 266*, 10246−10248.
54. Egawa, T., Miki, H., Ogura, T., Makino, R., Ishimura, Y., and Kitagawa, T. (1992) *FEBS Lett. 305*, 206−208.
55. Hosten, C. M., Sullivan, A. M., Palaniappan, V., Fitzgerald, M. M., and Terner, J. (1994) *J. Biol. Chem. 269*, 13966−13978.
56. Macdonald, I. D. G., Sligar, S. C., Christian, J. F., Unno, M., and Champion, P. M. (1999) *J. Am. Chem. Soc. 121*, 376−380.
57. Egawa, T., Proshlyakov, D. A., Miki, H., Makino, R., Ogura, T., Kitagawa, T., and Ishimura, Y. (2001) *J. Biol. Inorg. Chem. 6*, 46−54.

BI0118456